Biosynthesis of aurodox, a Type III secretion system inhibitor from *Streptomyces goldiniensis.*

Running Title: Characterisation of aurodox biosynthesis

Rebecca E McHugh[a,b] (Orcid 0000-003-4664-6125), John T Munnoch[a] (Orcid 0000-0002-9018-6026), Robyn E Braes[a], Iain J. W. McKean[a,c], Josephine M Giard[a] (Orcid 0000-0002-3376-7190), Andrea Taladriz-Sender[c], Frederik Peschke[c], Glenn A Burley[c], (Orcid 0000-0002-4896-113X), Andrew J Roe[b], & Paul A Hoskisson[a#] (Orcid 0000-0003-4332-1640).

[a] Strathclyde Institute of Pharmacy and Biomedical Sciences, University of Strathclyde, 161 Cathedral Street, Glasgow, G4 0RE, UK

[b] Institute of Infection, Immunity and Inflammation, University of Glasgow, Glasgow, G12 8TA, UK

[c] Department of Pure and Applied Chemistry, University of Strathclyde, 252 Cathedral Street, Glasgow, G1 1BX.

 # Correspondence: paul.hoskisson@strath.ac.uk

Word Count (Abstract): 213

Word Count (Total): 2939

Supplementary Data: McHugh et al., 2022 - Biosynthesis of aurodox, a Type III secretion system inhibitor from *Streptomyces goldiniensis*. Figshare. https://doi.org/10.6084/m9.figshare.19140005.v1

Abstract: The global increase in antimicrobial-resistant infections means that there is a need to develop new antimicrobial molecules and strategies to combat the issue. Aurodox is a linear polyketide natural product that is produced by *Streptomyces goldiniensis,* yet little is known about aurodox biosynthesis or the nature of the biosynthetic gene cluster (BGC) that encodes its production. To gain a deeper understanding of aurodox biosynthesis by *S. goldiniensis,* the whole genome of the organism was sequenced, revealing the presence of an 87 kb hybrid Polyketide Synthase/Non-Ribosomal Peptide Synthetase (PKS/NRPS) BGC. The aurodox BGC shares significant homology with the kirromycin BGC from *S. collinus* Tü 365; however, the genetic organisation of the BGC differs significantly. The candidate aurodox gene cluster was cloned and expressed in a heterologous host to demonstrate that it was responsible for aurodox biosynthesis and disruption of the primary PKS gene (*aurAI*) abolished aurodox production. These data support a model whereby the initial core biosynthetic reactions involved in aurodox biosynthesis follow that of kirromycin. Cloning *aurM** from *S. goldiniensis* and expressing this in the kirromycin producer *S. collinus* Tü 365 enabled methylation of the pyridone group, suggesting this is the last step in biosynthesis. This methylation step is also sufficient to confer the unique Type III Secretion System inhibitory properties to aurodox.

Importance: Enterohaemorrhagic *Escherichia coli* (EHEC) is a significant global pathogen for which traditional antibiotic treatment is not recommended. Aurodox inhibits the ability of EHEC to establish infection in the host gut through the specific targeting of the Type III Secretion System, whilst circumventing the induction of toxin production associated with traditional antibiotics. These properties suggest aurodox could be a promising anti-virulence compound for EHEC, which merits further investigation. Here, we have characterised the aurodox biosynthetic gene cluster from *Streptomyces goldiniensis* and have established the key enzymatic steps of aurodox biosynthesis that give rise to the unique anti-virulence activity. These data provide the basis for future chemical and genetic approaches to produce aurodox derivatives with increased efficacy and the potential to engineer novel elfamycins.

Keywords: *Streptomyces*, antibiotic, elfamycin, EHEC, polyketide

Introduction

Streptomyces bacteria are renowned for their ability to produce a plethora of natural products that exhibit a wide range of chemical structures, activities and modes of action (1). One such molecule is aurodox, which has a remarkable anti-virulence mode of action in addition to its well understood anti-gram-positive properties (2–4). Aurodox is produced by *Streptomyces goldiniensis* and belongs to the elfamycin group of antibiotics, which are characterised by their mode of action rather than their chemical structure (4). The anti-bacterial mode of action of the elfamycins is well understood, where they target protein translation through inhibition of Elongation Factor Thermo-unstable (EF-Tu; (4). Direct EF-Tu binding by kirromycin/aurodox-type elfamycins prevents EF-Tu:GDP from dissociating from the ribosome, preventing elongation and inhibiting protein synthesis (4). Aurodox also has an additional mode of action, originally discovered during a screen for Type III Secretion System (T3SS) inhibitors in Enteropathogenic *Escherichia coli* (EPEC; (5). More recently, it was demonstrated that aurodox inhibits T3SS and virulence in Enterohaemorrhagic *E. coli* (EHEC) and EPEC through an EF-Tu-independent mechanism, involving the downregulation of transcription of the master virulence regulator, Ler (6).

Aurodox was discovered in 1973 (2), it is a linear polyketide compound which is highly similar to kirromycin (7) differing only in methylation of the pyridone moiety. Kirromycin biosynthesis has been characterised and the BGC encodes five large polyketide synthase (PKS) units which act to form the polyketide backbone, before tailoring enzymes decorate the molecule (7–10). Given the similarity of the molecules, we hypothesised that the aurodox biosynthetic gene cluster (BGC) may be homologous to the hybrid PKS/Non-ribosomal peptide synthetase (NRPS) BGC of kirromycin, with the addition of an ORF responsible for pyridone-associated methylation (**Fig. 1**).

In EHEC infections, antibiotic treatment is not recommended due to the prevalence of systemic side effects (11, 12), and the upregulation of the bacterial SOS response in EHEC, resulting in Shiga toxin expression(13–16). The consequences of this are severe for patients with increased Shiga toxin levels being associated with systemic infections and nephrotoxicity (12).

Therefore, inhibiting virulence in a specific and targeted manner, that does not induce Shiga toxin production, represents a promising strategy for repurposing aurodox as an anti-virulence treatment (6).

Here, we present the identification and cloning of the aurodox BGC, followed by confirmation of the genes responsible for aurodox biosynthesis through heterologous expression and gene disruption. The aurodox biosynthetic cluster was found to differ in the organisation from that of kirromycin; however, based on homology, we proposed a biosynthetic scheme for aurodox. Additionally, we demonstrate, through heterologous expression of the putative methyltransferase (*aurM**), that methylation of the pyridone moiety is the last step in aurodox biosynthesis. This improved understanding of aurodox biosynthesis will enable greater exploitation and engineering of aurodox as an anti-virulence therapy and extends our knowledge of an important group of antimicrobial compounds.

Results

Whole Genome Sequencing of *S. goldiniensis* reveals a putative aurodox BGC with homology to the kirromycin BGC.

To identify the aurodox BGC, the whole genome of *S. goldiniensis* ATCC 21386 was sequenced using a hybrid-approach where Illumina, PacBio and Oxford Nanopore technologies were used to generate a high-quality draft genome (PRJNA602141; (17)). Analysis of the sequence using antiSMASH (18) identified 36 putative BGCs within the *S. goldiniensis* genome **(Supplementary Table S1;** (17)*.* A large region of the *S. goldiniensis* genome was identified (position 4,213,370 - 4,484,508; 271 kb) that was rich in BGCs including an 87 kb region with homology to the kirromycin BGC (7). This 87 kb region consisted of 25 ORFs, with 23 ORFs exhibiting >60% similarity to homologs in kirromycin BGC from *S. collinus* (**Table 1; Supplementary Table S2**). Despite the homologous ORFs within the BGCs, clear differences were apparent between the kirromycin and aurodox gene clusters, such as the inversion of NRPS/PKS genes and rearrangements of genes which encode the decorating enzymes of the polyketide backbone (**Fig. 2**). Two additional genes were identified in the aurodox BGC that lacked homologues in kirromycin cluster (**Table 1**). A gene encoding a SAM-dependant *O*-methyltransferase (*aurM**)*,* which we propose catalyses the addition of the methyl group to the pyridone moiety, and a hypothetical protein with no predicted homology to genes of known function (*aurQ*). Given the homology to the kirromycin BGC, it was hypothesised that this putative BGC was responsible for aurodox production in *S. goldiniensis* (**Table 1**).

Heterologous expression of the putative aurodox BGC in *Streptomyces coelicolor* M1152 results in aurodox biosynthesis.

To determine if the putative aurodox BGC was responsible for aurodox biosynthesis, a Phage Artificial Chromosome (PAC) library was constructed from *S. goldiniensis* genomic DNA, and the resulting pESAC-13A vectors (19) were screened for the presence of the putative aurodox cluster via PCR (Bio S & T, Canada; **Fig. S1;** Oligonucleotide primers can be found in **Supp**

Table S5). Two PCR positive PAC clones were identified which contained the entire region of interest, with one clone (pAur1) taken forward for further study (**Fig. S1, S2 & S3**). The complete PAC was sequenced to identify the boundaries of the pAur1, which contained a 129Kbp insert (See **Supp. File. pAur1**; **Fig. S2)** and the complete region proposed to encode the aurodox BGC.

Introduction of pAur1, which integrates at the ϕC31 integration site, to the *S. coelicolor* M1152 'superhost' was achieved via conjugation from the non-methylating ET12567/pR9604 strain to avoid the methyl-specific restriction system (20). Importantly, *S. coelicolor* M1152 encodes three copies of EF-Tu, including one copy of the elfamycin-resistant type EF-Tu, *tuf2* suggesting this strain would be a suitable host for expression of aurodox. Exconjugants containing the putative aurodox BGC (pAur1) and empty vector controls (pESAC-13A) were screened via PCR (**Fig. S3**) and the resulting strains were cultured in liquid media. Culture supernatant extracts were then subjected to LCMS analysis and compared to an authentic aurodox standard (**Fig. 3A)**. An equivalent aurodox peak was also observed in the trace from *S. goldiniensis* extract (**Fig. 3B**). Extracts from the *S. coelicolor* M1152/pESAC-13A, empty vector control lacked the distinct peak of aurodox (**Fig. 3C)**, whereas *S. coelicolor* M1152/pAur1, the strain containing the putative aurodox cluster, exhibited the characteristic peak (**Fig. 3D**). Mass spectrometric analysis revealed peaks at m/z 793, corresponding to the molecular ion of aurodox from cultures of *S. coelicolor* M1152/pAur1 and *S. goldiniensis*. This peak was absent from the empty vector control strain (**Fig. 3C),** indicating that the putative aurodox BGC encodes aurodox biosynthesis in *S. goldiniensis*.

To unequivocally confirm the role of the putative aurodox BGC genes encoded on the pAur1 clone, a deletion of the Type IPKS (*aurAI*) was performed using ReDirect (21), resulting in pAur1Δ*aurAI*. We hypothesised that the deletion of the primary PKS would prevent aurodox biosynthesis and confirm the putative BGC was required for aurodox biosynthesis. Analysis of extracts from *S. coelicolor* M1152/pAur1Δ*aurAI* lacked a peak at the aurodox-associated retention time (**Fig. 3E)** confirming the role of these genes in aurodox biosynthesis.

Bioassays of these culture supernatants using *Staphylococcus aureus* (ATCC 43300) as an indicator organism, further support the LCMS data, with *S. coelicolor* M1152/pAur1 inhibiting *S. aureus* growth, whereas the empty vector control (*S. coelicolor* M1152/pESAC-13A) and the deletion strain (*S. coelicolor* M1152/pAur1Δ*aurAI*) display reduced bioactivity (**Fig. 3F)**.

Proposed biosynthesis of aurodox follows that of kirromycin

The ClusterTools algorithm from antiSMASH was used to annotate the core PKS/NRPS genes of the aurodox BGC including specific module assignments (18, 22). This facilitated the prediction that the catalytic domains of AurI to AurVI largely follow those of KirI to KirVI of the kirromycin gene cluster despite the rearrangements in the overall cluster architecture (**Fig. 2 & 4;** (7, 9). In AurAI and AurAII, acetyl Co-A extension is via Claisen condensation reactions (8), however the PKSs are atypical in arrangement, with two additional dehydratase domains present. Whilst these were not previously identified in the kirromycin pathway(7), reanalysis of the kirromycin pathway using ClusterTools (22) does predict the presence of these domains in KirI to KirVI. Remarkably, no homolog of *kirP,* the kirromycin phosphopantheteinyl transferase (PPTase) was identified in the aurodox BGC.

It is predicted that *aurAIII* encodes a hybrid NRPS/PKS enzyme consisting of consecutive condensation and adenylation domains which catalyse the condensation of glycine and the incorporation of the amide bond, a process conserved with the kirromycin pathway. The enzymes AurAIV-AVII are predicted to extend the aurodox backbone before AurB (which possesses the conserved DTLQLGVIWK motif (23), catalyses the incorporation β-alanine, presumably synthesised by the putative aspartate-1-decarboxylase, AurD (**Fig. 4 & Table 1)**.

A SAM-dependent methyltrasferase, *aurM catalyses the conversion of kirromycin to aurodox.**

An additional SAM-dependant *O*-methyltransferase (AurM*) was identified in the aurodox BGC, which was absent in the kirromycin BGC. Preliminary analysis of the LCMS traces from fermentations of *S. goldiniensis* and *S. coelicolor* M1152/pAur1 indicated that small amounts

of kirromycin were present in samples, suggesting that the methylation of kirromycin may be the final step in aurodox biosynthesis. It was hypothesised that AurM* catalyses the conversion of kirromycin to aurodox. To test this, *aurM** from *S. goldiniensis* was cloned in to an integrating vector (pIJ6902; (24) and introduced in to *Streptomyces collinus* Tü 365, a natural kirromycin producer. Empty vector controls of *S. collinus* Tü 365 containing pIJ6902 showed no species corresponding to aurodox but did show the presence of kirromycin when compared to an authentic standards (**Fig. 5A & 5B)**. LCMS analysis of solvent extracts from *S. collinus* Tü 365 expressing *aurM** revealed characteristic peaks corresponding to aurodox and kirromycin (**Fig. 5C)**, with negative scan MS showing a m/z ratio of 793, corresponding to aurodox in addition to a m/z ratio 785 which corresponds to kirromycin **(Fig. 5A & Fig S5)**. This indicates that AurM* is responsible for the methylation of kirromycin as a precursor to aurodox formation.

Discussion

Understanding the mode of action, resistance mechanisms and the biosynthesis of useful natural products is key to their development for clinical application. The linear polyketide, aurodox, whilst being known for almost 50 years, was recently found to exhibit novel anti-virulence activity via a previously unknown target (6), yet nothing was known about its biosynthesis. Whilst aurodox is structurally similar to kirromycin, it is now well known that structurally identical or highly similar natural products can be biosynthesised via diverse chemical routes (1, 25–28), suggesting that there is still much to be learned from studying biosynthesis of structurally similar natural products in terms of novel activity and evolution of natural products.

Despite similarities in structure, anti-bacterial mode of action and core BGC machinery between aurodox and kirromycin, key differences in biosynthesis were identified. The aurodox cluster is ~80% similar to the kirromycin BGC, sharing 23 of the 25 genes, with seven genes within both clusters encoding hypothetical proteins with no assigned function. There is no apparent PPTase (*kirP* homolog) encoded in the aurodox cluster, which would normally post-

translationally modify the acyl carrier protein (ACP) to facilitate extension of the PK/NRP chains during assembly, suggesting that this function may be fulfilled by a promiscuous PPTase encoded elsewhere in the genome (29). Remarkably, no thioesterase domain was identified in the PKS-NRPS megasynthases. There is a putative Dieckmann-like cyclase encoded within the cluster (*aurB*), which may be responsible for the cleavage and cyclisation of the aurodox molecule, a mechanism that recently been proposed in a few other pyridone natural products (30). The anti-virulence activity of aurodox requires methylation of the pyridone ring, which is catalysed by *aurM**. The 'magic methyl' effect is well known in drug discovery for enhancing the activity and pharmacological properties of drugs (31, 32), and the kirromycin to aurodox transformation indicates that this has been exploited in nature to alter the activity of natural products. Moreover, this indicates that derivatisation of the pyridone ring of kirromycin may be a useful strategy for diversifying elfamycin activities. Regarding the origin of *aurM*,* two additional *O*-methyl transferases are encoded within the *S. goldiniensis* genome, each with ~35% amino acid similarly to AurM*, which may suggest that *aurM** was acquired by horizontal gene transfer (HGT) rather than duplication of an existing *O*-methyltransferase from the genome of *S. goldiniensis,* and offers insight in to the evolution of novel activities in natural products and the potential of this to be driven through HGT of single ORFs.

Overall, this greater understanding of biosynthesis of aurodox and the steps that contribute to unique modes of action will enable us to explore the potential of aurodox as a therapeutic agent for EHEC treatment in the food chain and the clinic.

Materials and Methods

Growth and Maintenance of Bacterial Strains.

The bacterial strains used in this study are detailed in **Table S3**. Genetic constructs used and their antibiotic selection are described in **Table S4**. Routine growth and maintenance procedures were carried out according to Kieser *et al,*(33). A list of oligonucleotides used in this study can be found in **Table S5**.

Whole Genome Sequencing *Streptomyces goldiniensis.*

Genomic DNA was extracted from *S. goldiniensis* using the Streptomyces DNA isolation protocol described by Kieser *et al,* (33). Nanopore reads were obtained using a genomic DNA library prepared in accordance with the Nanopore™ 1D ligation protocol, using MinION SPOT ON MK1 R9© flow cells and the raw data was converted to sequence data via MinKNOW base calling software. Illumina data was obtained from Microbes NG (Birmingham, UK) using the HiSeq 2500 sequencing platform. Reads were adapter trimmed using Trimmomatic 0.30 (34) with a sliding window quality cut off of Q15. PacBio sequencing was provided by Nu-omics at (University of Northumbria, UK) using the PacBio Sequel instrument and contigs were assembled in HGAP4.

Streptomyces goldiniensis genome was assembled using SPAdes (34) using data provided by all three platforms. AutoMLST (35) was used to determine the closest neighbour *S. bottropensis* ATCC 25435 (Taxonomy ID: 1054862) which was used for scaffold-based assembly via MeDuSa(36), with quality analysis carried out using QUAST (37). Annotation of the *Streptomyces goldiniensis* genome was created using Prokka (38) and can be accessed at the Genbank Bioproject PRJNA602141. Biosynthetic gene cluster identification was carried out using antiSMASH bacterial version 5.0.0 with modular enzymatic domains analysis carried out using the PKS/NRPS domain annotation function in antiSMASH (18).

Aurodox production, purification and detection.

Streptomyces spore stocks (1 x 10^8 spores) were pre-germinated in 10 ml of GYM medium (32) overnight at 30 ^{o}C with shaking at 250 rpm. Cells were then washed three times to remove

antibiotics (if used) and resuspended in 1ml of GYM, which was used to inoculate a 50 ml seed culture of GYM which were incubated at 30 ˚C with shaking at 250 rpm. After seven days, biomass was removed by centrifugation (4000 x *g*, 10 minutes) and culture supernatant was filter sterilised through a 0.2 µM Millipore™ filter. Supernatants were mixed with equal volume of chloroform and a separation funnel was used to remove the lower, solvent phase. Solvent extracts were dried under nitrogen and extracts were solubilised in ethanol for LC-MS analysis. Authentic aurodox standard (1 mg/ml) was purchased from Enzo (New York, USA). LC-MS was carried out on an Aglient 1100 HPLC instrument in conjunction with a Waters Micromass ZQ 2000/4000 mass detector. Electrospray ionization (ESI) was used in all cases. The RP-HPLC analysis was conducted on a Zorbax 45mm x 150mm C18 column at 40˚C. Ammonium acetate buffers were used as follows: Buffer A (5 mM Ammonium acetate in Water) and Buffer B (5mM Ammonium acetate in acetonitrile). Positive and negative electrospray methods were applied with of 100 to 1000 AMU positive, 120-1000 AMU negative with a scanning time of 0.5 seconds. The UV detection was carried out at 254 nm.

Construction of aurodox expression strains and deletion mutant.

Aurodox encoding vector pAur1 (Bio S & T, Canada) and empty vector pESAC-13A (39) were transferred to the non-methylating *Escherichia coli* strain ET12567 via tri-parental mating. Briefly, fresh overnight cultures of *E. coli* DH10β containing pAur1 or the parental vector pESAC-13A (apramycin resistant), *E. coli* Top10 containing the driver plasmid pR9604 (Beta-lactam resistant) and ET12567 (Chloramphenicol resistant) were grown to an OD_{600} of 0.6. Cells were washed three times in fresh LB by centrifugation at 4000 x *g* and resuspended in 1 ml of LB. A 20 µl aliquot of each strain was plated in the centre of a LB plate and incubated at 37 ˚C overnight. The resulting growth was re-streaked on to the required antibiotic selection and the presence of the conjugating vector in the *E. coli* ET12567/pR9604 strain was confirmed via colony PCR. Mutation in pAur1 were carried out according to the ReDirect PCR targeting system in *Streptomyces* (21), using the hygromycin resistance cassette, pIJ10700 as the disruption cassette (http://streptomyces.org.uk/redirect/RecombineeringFEMSMP-2006-5.pdf). Disrupted PACs were introduced in to *E. coli* ET12567/pR9604 via tri-parental mating

297 and subsequently moved into *Streptomyces coelicolor* M1152 via conjugation as described
298 above.

299 **Cloning of *aurM** from *Streptomyces goldiniensis.***

300 The putative *O*-methyltransferase *aurM** was amplified from *S. goldiniensis* genomic DNA
301 using the oligonucleotide primers in **Table S5** and cloned in to pIJ6902 using the NEB Gibson
302 Assembly cloning kit (24). Conjugation of pIJ6902 based vectors was according to Kieser et
303 al., (33).

304 **Bioassays**

305 Bioassays were conducted using disc diffusion assays with *Streptomyces* fermentation
306 extracts on soft nutrient overlays containing *Staphylococcus aureus* ATCC43300 as the
307 indicator organism.

308

Funding Information

We would like to thank the University of Strathclyde and University of Glasgow for jointly funding the PhD of REM. AJR & PAH would like to acknowledged funding from MRC (MR/V011499/1). PAH would also like to acknowledge funding from BBSRC (BB/T001038/1 and BB/T004126/1) and the Royal Academy of Engineering Research Chair Scheme for long term personal research support (RCSRF2021\11\15).

Funding Statement

The funders had no role in study design, data collection and interpretation, or the decision to submit the work for publication

Acknowledgements

We would like to thank Professor Wolfgang Wohlleben (University of Tübingen) for the gift of the *Streptomyces collinus* Tü 365 strain, Dr Margherita Sosio (Naicons) for the gift of pESAC-13A and Professor Mervyn Bibb (John Innes Centre) for the gift of the *S. coelicolor* M1152 strain. We would also like to thank Professor Iain S. Hunter (University of Strathclyde) and Professor Matt Hutchings (John Innes Centre) for helpful discussions.

References

1. Chevrette MG, Gutiérrez-García K, Selem-Mojica N, Aguilar-Martínez C, Yañez-Olvera A, Ramos-Aboites HE, Hoskisson PA, Barona-Gómez F. 2019. Evolutionary dynamics of natural product biosynthesis in bacteria. Nat Prod Rep 37:566-599..

2. Berger J, Lehr HH, Teitel S, Maehr H, Grunberg E. 1973. A new antibiotic X-5108 of *Streptomyces* origin. Journal of Antibiotics 26:15–22.

3. Vogeley L, Palm GJ, Mesters JR, Hilgenfeld R. 2001. Conformational Change of Elongation Factor Tu (EF-Tu) Induced by Antibiotic Binding crystal structure of the complex between EF-Tu·GDP and aurodox. J Biol Chem 276:17149–17155.

4. Prezioso SM, Brown NE, Goldberg JB. 2017. Elfamycins: inhibitors of elongation factor-Tu. Mol Microbiol 106:22–34.

5. Kimura K, Iwatsuki M, Nagai T, Matsumoto A, Takahashi Y, Shiomi K, Ōmura S, Abe A. 2010. A small-molecule inhibitor of the bacterial type III secretion system protects against *in vivo* infection with *Citrobacter rodentium*. J Antibiotics 64:197–203.

6. McHugh RE, O'Boyle N, Connolly JPR, Hoskisson PA, Roe AJ. 2018. Characterization of the Mode of Action of Aurodox, a Type III Secretion System Inhibitor from *Streptomyces goldiniensis*. Infect Immun 87.

7. Weber T, Laiple KJ, Pross EK, Textor A, Grond S, Welzel K, Pelzer S, Vente A, Wohlleben W. 2008. Molecular Analysis of the Kirromycin Biosynthetic Gene Cluster Revealed β-Alanine as Precursor of the Pyridone Moiety. Chemistry & Biology 15:175-188.

8. Robertsen HL, Musiol-Kroll EM, Ding L, Laiple KJ, Hofeditz T, Wohlleben W, Lee SY, Grond S, Weber T. 2018. Filling the Gaps in the Kirromycin Biosynthesis: Deciphering the Role of Genes Involved in Ethylmalonyl-CoA Supply and Tailoring Reactions. Sci Rep 8:3230.

349 9. Laiple KJ, Härtner T, Fiedler H-P, Wohlleben W, Weber T. 2009. The kirromycin gene
350 cluster of *Streptomyces collinus* Tü 365 codes for an aspartate-α-decarboxylase, KirD, which
351 is involved in the biosynthesis of the precursor β-alanine. J Antibiotics 62:465–468.

352 10. Pavlidou M, Pross EK, Musiol EM, Kulik A, Wohlleben W, Weber T. 2011. The
353 phosphopantetheinyl transferase KirP activates the ACP and PCP domains of the kirromycin
354 NRPS/PKS of *Streptomyces collinus* Tü 365. Fems Microbiol Lett 319:26–33.

355 11. Deng W, Puente JL, Gruenheid S, Li Y, Vallance BA, Vázquez A, Barba J, Ibarra JA,
356 O'Donnell P, Metalnikov P, Ashman K, Lee S, Goode D, Pawson T, Finlay BB. 2004.
357 Dissecting virulence: Systematic and functional analyses of a pathogenicity island. P Natl
358 Acad Sci Usa 101:3597–3602.

359 12. Goldwater PN, Bettelheim KA. 2012. Treatment of enterohemorrhagic *Escherichia coli*
360 (EHEC) infection and hemolytic uremic syndrome (HUS). Bmc Med 10:12.

361 13. Huerta-Uribe A, Marjenberg ZR, Yamaguchi N, Fitzgerald S, Connolly JPR, Carpena N,
362 Uvell H, Douce G, Elofsson M, Byron O, Marquez R, Gally DL, Roe AJ. 2016. Identification
363 and Characterization of Novel Compounds Blocking Shiga Toxin Expression in *Escherichia*
364 *coli* O157:H7. Front Microbiol 7:1930.

365 14. Melton-Celsa AR. 2014. Shiga Toxin (Stx) Classification, Structure, and Function.
366 Microbiol Spectr 2:EHEC-0024-2013.

367 15. Nguyen Y, Sperandio V. 2012. Enterohemorrhagic *E. coli* (EHEC) pathogenesis. Front
368 Cell Infect Mi 2:90.

369 16. Fuchs S, Mühldorfer I, Donohue-Rolfe A, Kerényi M, Emödy L, Alexiev R, Nenkov P,
370 Hacker J. 1999. Influence of RecA on *in vivo* virulence and Shiga toxin 2 production in
371 *Escherichia coli* pathogens. Microb Pathogenesis 27:13–23.

372 17. McHugh RE, Munnoch JT, Roe AJ, Hoskisson PA. 2021. Genome sequence of the
373 aurodox-producing bacterium *Streptomyces goldiniensis* ATCC 21386. Biorxiv
374 2021.06.01.446637.

375 18. Blin K, Shaw S, Steinke K, Villebro R, Ziemert N, Lee SY, Medema MH, Weber T. 2019.
376 antiSMASH 5.0: updates to the secondary metabolite genome mining pipeline. Nucleic Acids
377 Res 47:W81–W87.

378 19. Sosio M, Giusino F, Cappellano C, Bossi E, Puglia AM, Donadio S. 2000. Artificial
379 chromosomes for antibiotic-producing actinomycetes. Nat Biotechnol 18:343–345.

380 20. Paget MS, Chamberlin L, Atrih A, Foster SJ, Buttner MJ. 1999. Evidence that the
381 extracytoplasmic function sigma factor sigmaE is required for normal cell wall structure in
382 *Streptomyces coelicolor* A3(2). Journal of bacteriology 181:204–11.

383 21. Gust B, Challis GL, Fowler K, Kieser T, Chater KF. 2003. PCR-targeted *Streptomyces*
384 gene replacement identifies a protein domain needed for biosynthesis of the sesquiterpene
385 soil odor geosmin. Proceedings of the National Academy of Sciences of the United States of
386 America 100:1541–6.

387 22. Santos EL de los, Challis G. 2019. clusterTools: functional element identification for the in
388 silico prioritization of biosynthetic gene clusters. Access Microbiol 1.A1.

389 23. Rausch C, Weber T, Kohlbacher O, Wohlleben W, Huson DH. 2005. Specificity prediction
390 of adenylation domains in nonribosomal peptide synthetases (NRPS) using transductive
391 support vector machines (TSVMs). Nucleic Acids Res 33:5799–5808.

392 24. Huang J, Shi J, Molle V, Sohlberg B, Weaver D, Bibb MJ, Karoonuthaisiri N, Lih C, Kao
393 CM, Buttner MJ, Cohen SN. 2005. Cross-regulation among disparate antibiotic biosynthetic
394 pathways of *Streptomyces coelicolor*. Molecular Microbiology 58:1276–1287.

395 25. Jensen PR. 2016. Natural Products and the Gene Cluster Revolution. Trends Microbiol
396 24:968–977.

397 26. Kim SY, Ju K-S, Metcalf WW, Evans BS, Kuzuyama T, Donk WA van der. 2012. Different
398 Biosynthetic Pathways to Fosfomycin in *Pseudomonas syringae* and *Streptomyces* Species.
399 Antimicrob Agents Ch 56:4175–4183.

400 27. Sit CS, Ruzzini AC, Arnam EBV, Ramadhar TR, Currie CR, Clardy J. 2015. Variable
401 genetic architectures produce virtually identical molecules in bacterial symbionts of fungus-
402 growing ants. Proc National Acad Sci 112:13150–13154.

403 28. Grenade NL, Howe GW, Ross AC. 2021. The convergence of bacterial natural products
404 from evolutionarily distinct pathways. Curr Opin Biotech 69:17–25.

405 29. Beld J, Sonnenschein EC, Vickery CR, Noel JP, Burkart MD. 2013. The
406 phosphopantetheinyl transferases: catalysis of a post-translational modification crucial for life.
407 Nat Prod Rep 31:61–108.

408 30. Gui C, Li Q, Mo X, Qin X, Ma J, Ju J. 2015. Discovery of a New Family of Dieckmann
409 Cyclases Essential to Tetramic Acid and Pyridone-Based Natural Products Biosynthesis. Org
410 Lett 17:628–631.

411 31. McKean IJW, Hoskisson PA, Burley GA. 2020. Biocatalytic Alkylation Cascades: Recent
412 Advances and Future Opportunities for Late-Stage Functionalization. Chembiochem 21:2890–
413 2897.

414 32. McKean IJW, Sadler JC, Cuetos A, Frese A, Humphreys LD, Grogan G, Hoskisson PA,
415 Burley GA. 2019. S -Adenosyl Methionine Cofactor Modifications Enhance the Biocatalytic
416 Repertoire of Small Molecule C -Alkylation. Angewandte Chemie Int Ed 58:17583–17588.

417 33. Kieser T, Bibb M, Buttner M, Chater K, Hopwood, DA. 2000. Practical *Streptomyces*
418 Genetics. John Innes Foundation.

419 34. Bankevich A, Nurk S, Antipov D, Gurevich AA, Dvorkin M, Kulikov AS, Lesin VM, Nikolenko
420 SI, Pham S, Prjibelski AD, Pyshkin AV, Sirotkin AV, Vyahhi N, Tesler G, Alekseyev MA,
421 Pevzner PA. 2012. SPAdes: A New Genome Assembly Algorithm and Its Applications to
422 Single-Cell Sequencing. J Comput Biol 19:455–477.

423 35. Alanjary M, Steinke K, Ziemert N. 2019. AutoMLST: an automated web server for
424 generating multi-locus species trees highlighting natural product potential. Nucleic Acids Res
425 47:W276–W282.

426 36. Bosi E, Donati B, Galardini M, Brunetti S, Sagot M-F, Lió P, Crescenzi P, Fani R, Fondi
427 M. 2015. MeDuSa: a multi-draft based scaffolder. Bioinformatics 31:2443–2451.

428 37. Gurevich A, Saveliev V, Vyahhi N, Tesler G. 2013. QUAST: quality assessment tool for
429 genome assemblies. Bioinformatics 29:1072–1075.

430 38. Seemann T. 2014. Prokka: rapid prokaryotic genome annotation. Bioinformatics 30:2068–
431 2069.

432 39. Sosio M, Bossi E, Donadio S. 2001. Assembly of large genomic segments in artificial
433 chromosomes by homologous recombination in *Escherichia coli*. Nucleic Acids Res 29:e37–
434 e37.

435

436 **Figure Legends**

437 **Figure 1: Chemical structures of the elfamycins kirromycin and aurodox.** Red box
438 highlights the additional methylation site of aurodox located on the pyridone ring.

439 **Figure 2: Comparison of aurodox and kirromycin gene clusters.** Adjoining lines represent
440 amino acid similarity according to scale. Grey genes represent non-homologous genes, *
441 represents the SAM-dependant *O*-methyltransferase AurM*. Figure generated by clinker.py
442 using (GCA_018728545.1).

443 **Figure 3: Heterologous expression of aurodox biosynthesis in *Streptomyces coelicolor***
444 **M1152.** Chromatograms of aurodox standard (Enzo; **A**). Peak at aurodox retention time is
445 indicated. **(B)** Chromatogram from Wild-Type *Streptomyces goldiniensis* indicating aurodox
446 production. **(C)** Chromatogram from the empty vector (pESAC-13A) control strain *S. coelicolor*
447 M1152, indicating the absence of an aurodox-associated peak. **(D)** Chromatogram of extract
448 from growth of *S. coelicolor* M1152/pAur1. Aurodox peak is visible at 7.12 min, and the MS
449 data indicate the presence of aurodox. (**E**) Chromatogram of extracts from *S. coelicolor*
450 M1152/pAur1Δ*aurA*1 showing absence of an aurodox-associated peak. Corresponding MS
451 data can be found in **Fig. S4**. **(E)** Bioactivity of the extracts used in **A-E**, indicating the zones
452 of inhibition associated with the extracts by disc diffusion against *Staphylococcus aureus*
453 ATCC 43300.

454 **Figure 4: Summary of the enzymatic reactions carried out by AurAI-AurAVII lin aurodox**
455 **PKS backbone biosynthesis.** ACP: acyl carrier protein; AT: acyltransferase domain; C:
456 condensation domain; DH: dehydratase domain ER: enoyl reductase domain; KR: keto
457 reductase domain; KS: keto synthase domain; MT: methyl transferase domain; PCP: peptidyl
458 carrier protein; TAD: trans-AT docking domain

459

460 **Figure 5: Methylation of kirromycin is the last step in aurodox biosynthesis and is**
461 **catalysed by AurM*.** Chromatograms of aurodox **(A)** and kirromycin **(B)** standards and
462 fermentation extracts from a control strain *S. collinus* Tü 365 containing pIJ6902 (empty vector
463 control; **C**) showing presence of kirromycin and absence of aurodox-associated mass and **(D)**
464 chromatogram from extracts from *S. collinus* Tü 365 containing pIJ6902_AurM* showing the
465 presence of aurodox with a retention time of 7.64 min. Corresponding MS data can be found
466 in **Fig. S5**.

467

468 **Table 1: Comparison of aurodox and kirromycin BGC and their functions**. Genes found
469 only in the aurodox cluster are in bold. To be consistent with kirromycin biosynthesis we have
470 maintained the nomenclature between this putative aurodox genes and their kirromycin
471 homologs.

Gene	kirromycin BGC Homolog	% homology of aurodox gene with its kirromycin homolog	Function
aurQ	**N/A**	**-**	**Hypothetical protein**
aurHV	*kirHV*	98%	Hypothetical protein
aurHVI	*kirHVI*	97%	Hypothetical protein
aurB	*kirB*	98%	Non-Ribosomal Peptide Synthetase
aurM*	**N/A**	**-**	**Type I SAM-dependant *O*-Methyltransferase**
aurCI	*kirCI*	97%	S-malonyltransferase
aurOII	*kirOII*	100%	Cytochrome P450 hydroxylase
aurD	*kirD*	97%	Aspartate 1-decarboxylase
aurM	*kirM*	99%	Class I SAM-dependent *O*-methyltransferase
aurCII	*kirCII*	96%	Ethylmalonyl-transferase
aurX	*kirX*	98%	Dieckmann cyclase
aurHII	*kirHIII*	95%	DUF3037 domain-containing protein
aurN	*kirN*	97%	Crotonyl-CoA carboxylase/reductase
aurIVI	*kirHIV*	92%	Magnesium ATP-ase
aurAI	*kirAI*	100%	Type 1 Polyketide Synthase
aurAII	*kirAII*	94%	Trans-AT PKS
aurAIII	*kirAIII*	99%	Non-ribosomal peptide synthetase
aurAIV	*kirAIV*	99%	Trans-AT PKS
aurAV	*kirAV*	99%	SDR family NAD(P)-dependent oxidoreductase
aurAVI	*kirAVI*	94%	Type I PKS
aurR	*kirRI/RII*	56%	TetR/AcrR family transcriptional regulator
aurOI	*kirOI*	97%	Cytochrome p450 hydroxylase
aurHI	*kirHI*	98%	Phytanoyl-CoA Dioxygenase

Fig 1

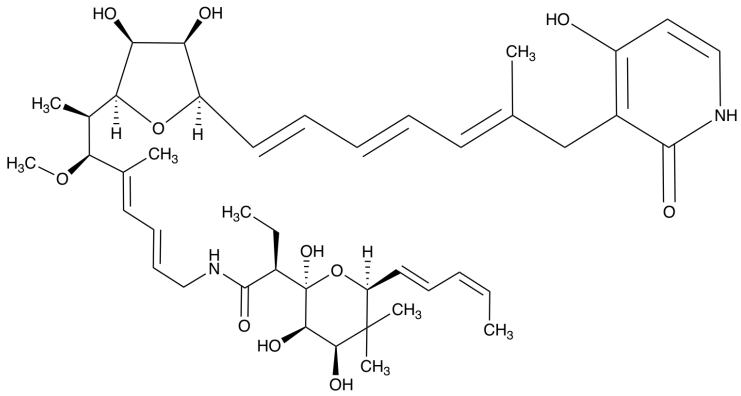

Kirromycin

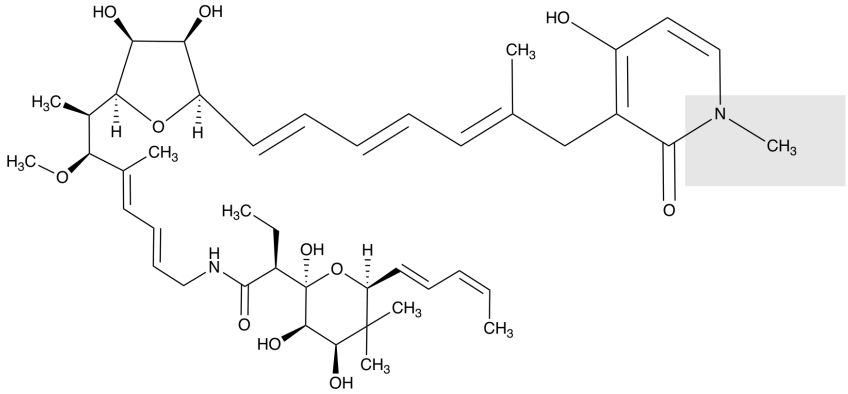

Aurodox

Figure 2

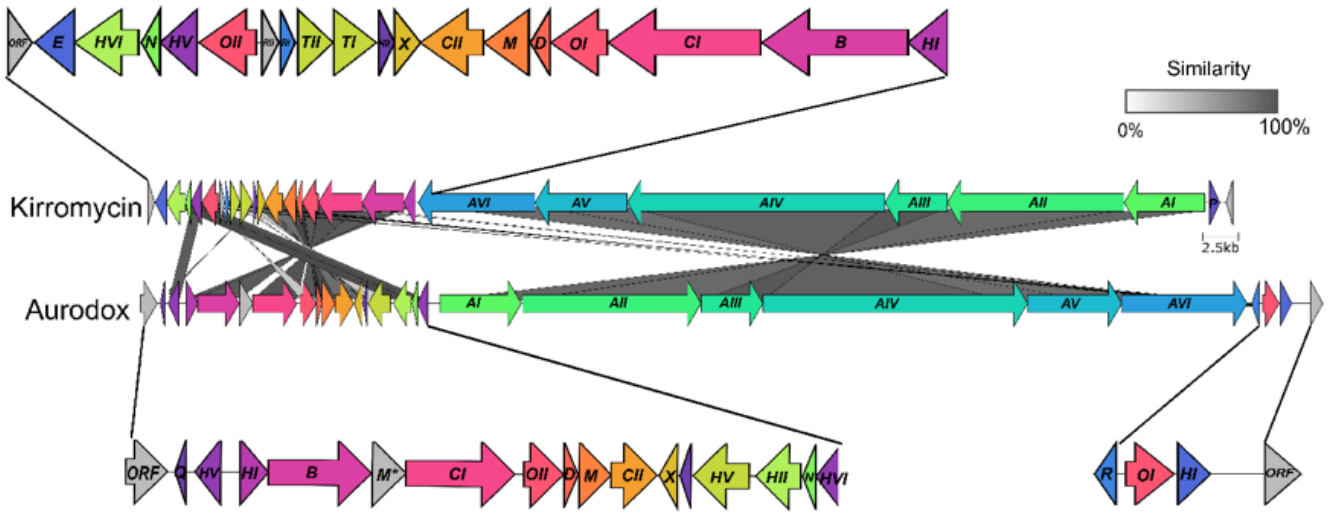

478 **Figure 3**

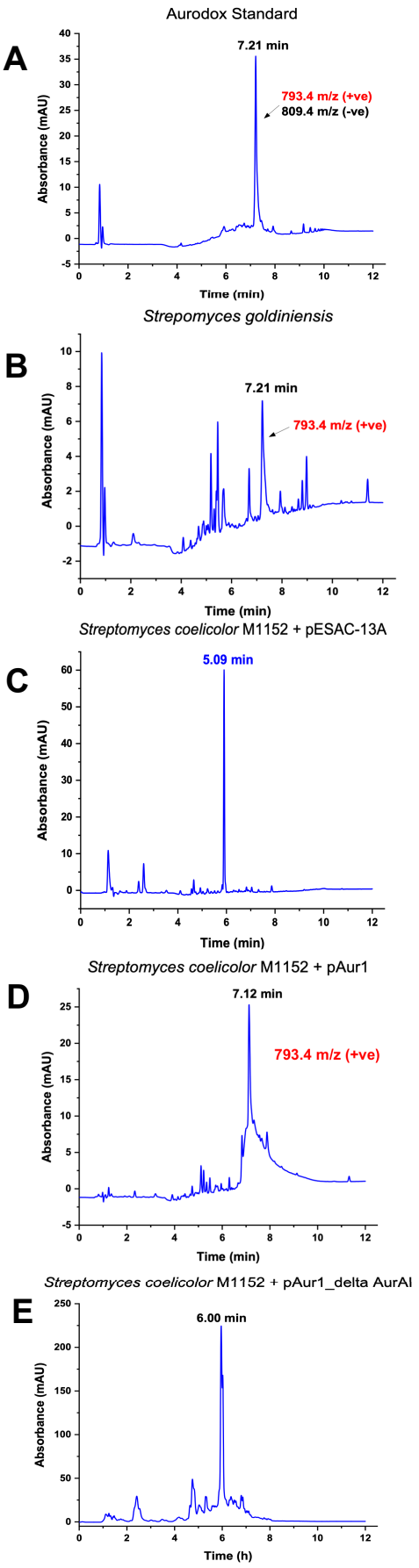

479

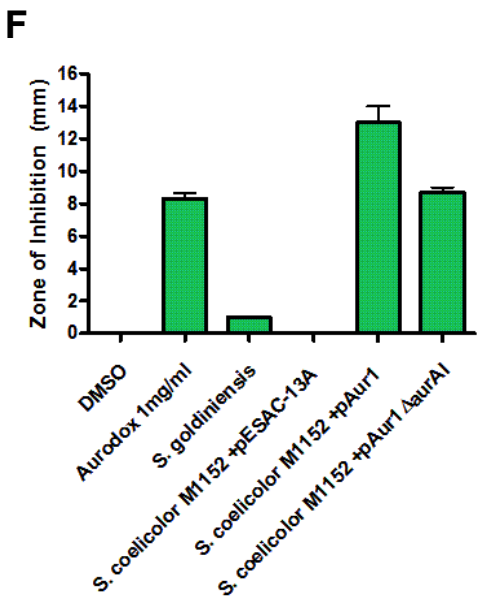

480 **Figure 4**

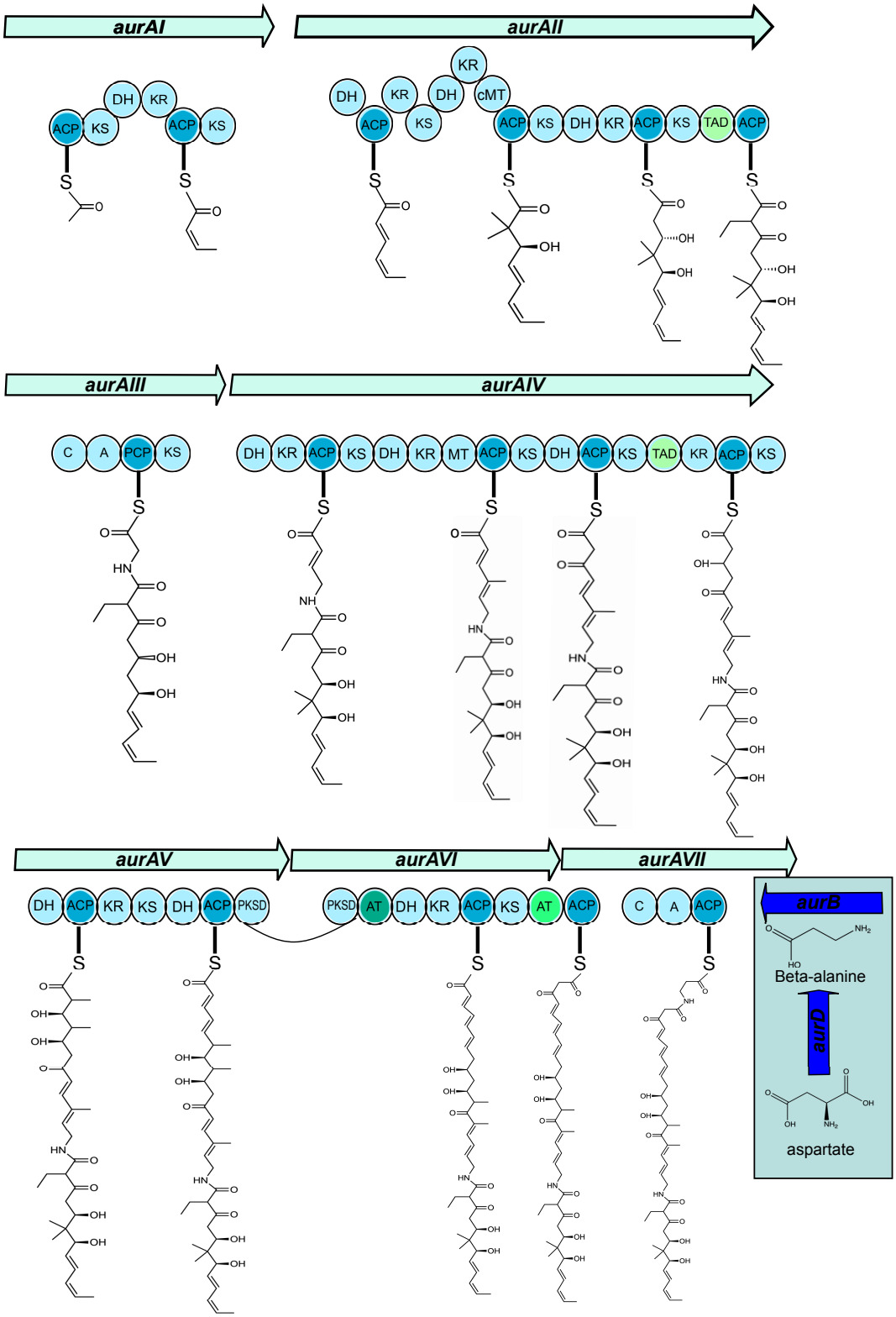

481

482

483

484 **Figure 5**

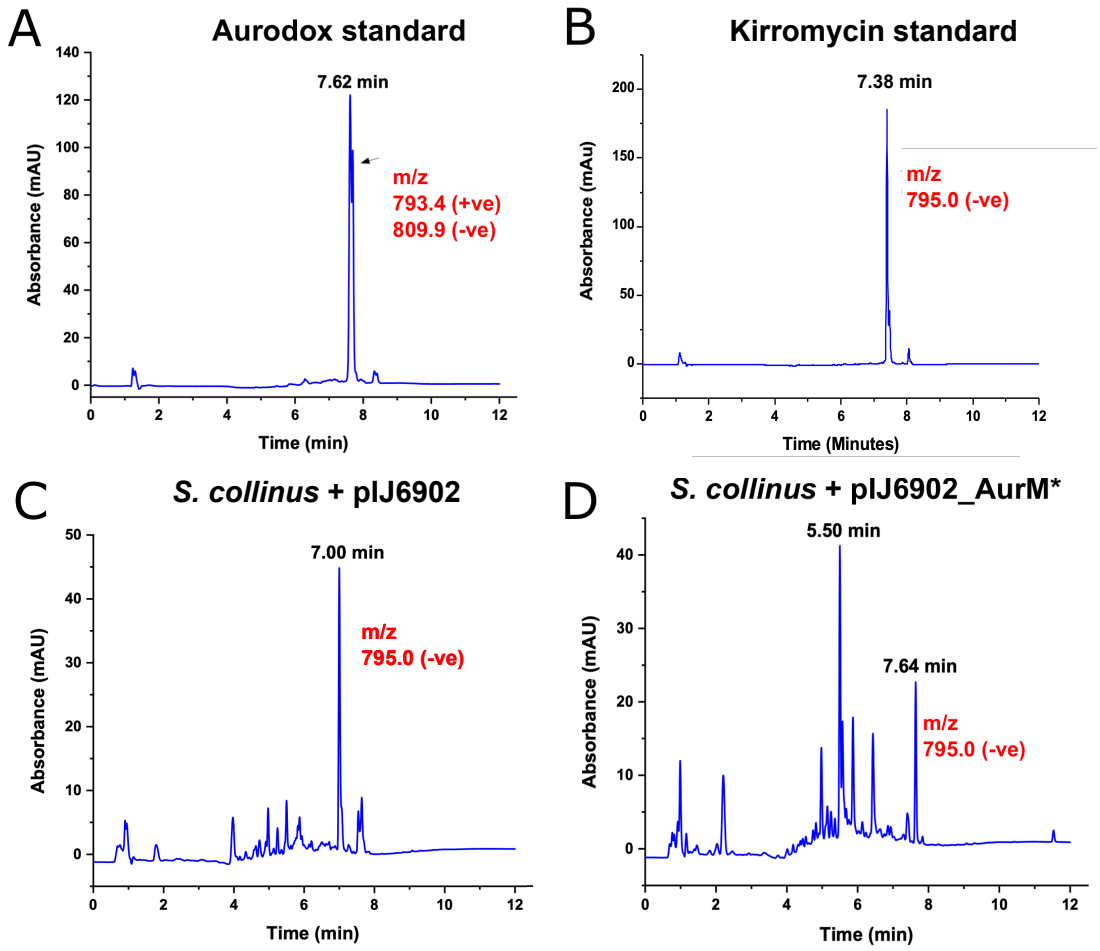

485

486